Proceedings 10th NUMGE 2023
10th European Conference on Numerical Methods in Geotechnical Engineering
Zdravkovic L, Kontoe S, Taborda DMG, Tsiampousi A (eds)

https://doi.org/10.53243/NUMGE2023-425

Effect of drawdown velocity on the stability of a small earth dam

M. Tretola[1], S. Sica[1]

[1]*Department of Civil Engineering, University of Sannio, Benevento, IT*

ABSTRACT: The paper describes the numerical procedure developed to investigate the effects of different drawdown rates on the stability of a zoned earth dam. A rapid lowering of the reservoir may be necessary to deal with an emergency condition immediately after an earthquake, but this operation could generate harmful effects on the stability of a dam if compromised by a previous seismic event. The selected case study represents the prototype of a small earth dam, i.e. a dam that for combination of its embankment height and water stored by the reservoir is not categorized as large. Unfortunately, unlike the large dams for which very strict controls are imposed by the ministerial technical departments, the small earth dams are less controlled even if the risk associated with them could be as high as for the larger ones. Through a 3-phase numerical approach, solved by the finite element method, different drawdown scenarios were simulated and their effects on the stability of a small dam prototype were quantified to identify the drawdown procedures that should be avoided before and soon after a strong seismic event.

Keywords: Zoned earth dam; drawdown; global instability mechanism

1 INTRODUCTION

In the field earth dams, caution should be paid to the fast drawdown of the reservoir especially if a strong earthquake occurred. The drawdown rate, combined to dam geometry and to the physical-mechanical properties of the embankment soils, might generate unstable conditions in the upstream shell up to partial or complete collapse of the embankment.

For dams located in seismic prone areas, on the other hand, it may be necessary to carry out a rapid emergency lowering of the reservoir to inspect the structure and possibly carry out repairs to protect the downstream population. While strict protocols exist for large dams forcing dam owners to slowly lower the reservoir, for small dams these restrictions could be dangerously circumvented. As well-known, the fast decrease of the reservoir water represents for the upstream shell (and the reservoir slopes) an abrupt change of pore water pressures inside the dam body. If the drawdown is too fast and its duration is much shorter than necessary to ensure drainage of the soil, excess pore water (e.p.w.) pressures may develop inside the dam body. If high e.p.w. pressures do not dissipate synchronously with the removal of the external water, slope failure is likely to occur.

Establishing the maximum drawdown rate that may safely be carried out is a crucial matter especially for dams placed in seismic areas (Sica et al., 2019).

The paper aimed to assess the effect of different drawdown scenarios on the global stability of a small zoned earth dam, which represents plenty of small or tailing dams present worldwide.

The numerical study was performed by means of a coupled approach, based on a 3-phase mathematical formulation implemented in the finite element (f.e.) commercial code Plaxis2D (Bentley, 2022). After simulating the embankment construction, the reservoir impounding and the seismic stages were modelled. The drawdown scenario was imposed soon after the earthquake stage. However, to unravel the role of the seismic event on dam stability, also a rapid lowering of the water level before the seismic stage was simulated.

2 PROTOTYPE DESCRIPTION

Figure 1 shows the cross section of an ideal small dam analysed in this study. It is a 13m-high zoned earth dam founded on a rigid base, with a central vertical clayey core (PI = 10%) and sandy shells. The shells are assumed to be made of sandy soils with a relative density as high as 80%.

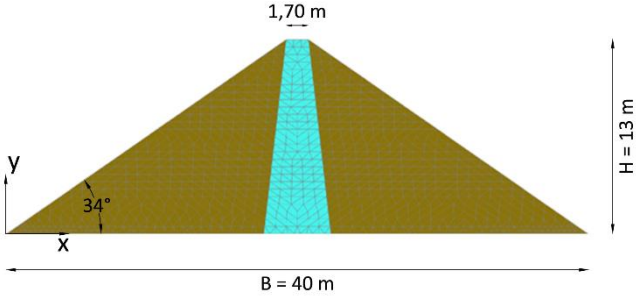

Figure 1. Small dam analysed.

Actually, the dam in Figure 1 recalls the prototype of many small earth dams built in Italy in the first half of the last century. Most of these dams were built before the seismic classification of the national territory and designed without considering or underestimating the seismic actions.

The dam was discretized by finite elements and assuming plane strain conditions. The constitutive law attributed to the dam soils is the *Hardening Soil with Small Strain Stiffness* (HS-small) implemented in Plaxis2D. This model is able to describe with sufficient accuracy the non-linear, hysteretic and plastic behaviour of the soil from the small to the high strain levels. Table 1 summarizes the constitutive parameters attributed to the core and the shells. The calibration of the constitutive parameters was performed through the *Soil Test* routine available in the software, which seeks the best-fitting between numerical and experimental results provided by lab tests for clays (oedometric, triaxial compression, and, if available, resonant column and cyclic torsional shear tests) or literature indications for sands.

Table 1. HS-small parameters used in the numerical analysis.

		Clayey core	Sandy shell
γ_{sat}	*[kN/m³]*	22	19.6
γ_{unsat}	*[kN/m³]*	21	16.3
e	*[-]*	0.4	0.6
k_{sat}	*[m/s]*	2.8E-10	3.5E-5
c’	*[kPa]*	14	1
φ’	*[°]*	36	41
ψ	*[°]*	0	0
k_0	*[-]*	0.4	0.34
E_{50}^{ref}	*[MPa]*	8.5	19.8
E_{oed}^{ref}	*[MPa]*	5.5	14.
E_{ur}^{ref}	*[MPa]*	25.5	59.4
m	*[-]*	0.98	0.5
G_0^{ref}	*[MPa]*	95	165
$\gamma_{0,7}$	*[-]*	1.7E-4	1.7E-4

To account for the partial saturation of the dam soils, a three-phase formulation was adopted by assigning to the core and the shells materials water retention curves retrieved from literature (Alonso and Pinyol, 2016; Sica et al., 2019) for fine and coarse soils, respectively (Figure 2 and Figure 3). The experimental curves were reproduced trough the Van Genuchten (1980) formulation reported in Eq. 1:

$$S(\psi) = S_{res} + (S_{sat} - S_{res})[1 + (g_a|\psi|)^{g_n}]^{g_c} \quad (1)$$

where $\psi = -\frac{p_w}{\gamma_w}$ represents the pore water pressure divided by the specific weight of water; S_{res} and S_{sat} are the degree of residual and complete saturation, respectively; g_n, g_a, g_c are empirical parameters calibrated on the selected experimental water retention curves.

Table 2. Van Genuchten model parameters.

		Clayey core	Sandy shell
S_{res}	*[-]*	0.46	0.08
S_{sat}	*[-]*	1.00	1.00
g_n	*[-]*	1.57	7.13
g_a	*[1/m]*	0.09	6.70
g_l	*[-]*	-5.00	0.50

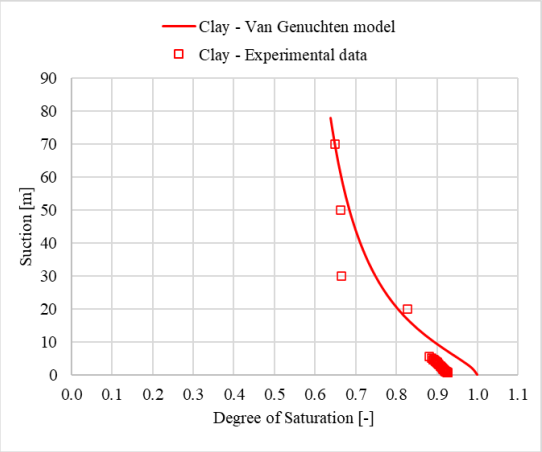

Figure 2. Water retention curve assumed for the core.

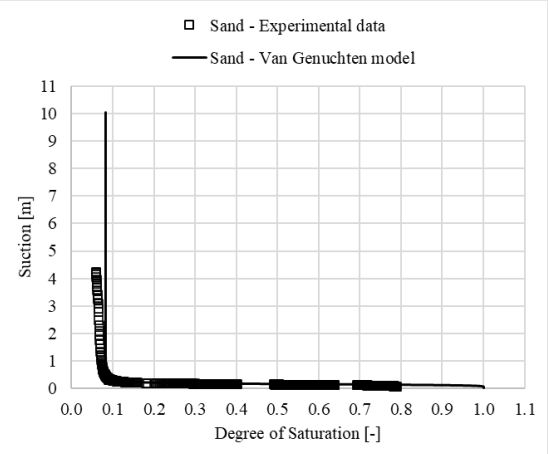

Figure 3. Water retention curve assumed for the shells.

3 NUMERICAL PROCEDURE

All the performed analyses may be divided into two groups: analyses in which the different drawdown scenarios were imposed during the static stage of the dam lifetime and analyses in which the drawdown scenario was activated soon after the seismic stage in order to assess dam safety to a sequence of dangerous phenomena (earthquake and drawdown).

3.1 Embankment construction stage

The first step of the computation process was the simulation of the embankment construction with a rate of 0.5 m/day under partially saturated conditions. A coupled analysis (*Consolidation* procedure in Plaxis2D) was performed in order to carry out a time-dependent analysis. As the hydraulic conditions concern, an initial degree of

saturation of 0.163 and 0.86 were imposed to the shells and the core, respectively. In this stage, elementary boundary conditions at the bottom of the analysis domain (*fully fixed*) were imposed as the dam was assumed to be founded on rigid rock.

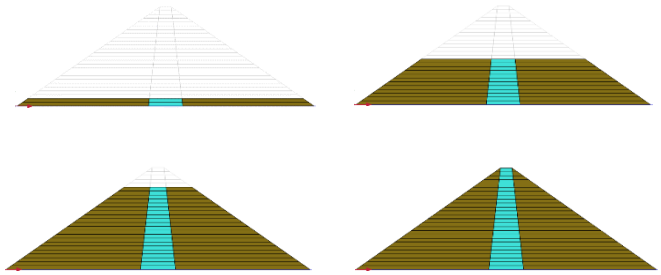

Figure 4. Staged construction simulation.

3.2 Impounding stage

Once the dam embankment was completely built, the post-construction consolidation stage and the first impounding of the dam were simulated. The reservoir was modelled by applying a water head of 11 m along the upstream face of the dam and the steady-state groundwater flow conditions. Figure 5a shows the active pore water pressures, p_{active}, computed in the dam body at the end of the first filling stage. Since a three-phase formulation has been adopted, the active pore water pressures are linked to the effective saturation S_{eff} of the soil and to the pore water pressure, p_{water}, according to Eq. 2:

$$p_{active} = S_{eff} \cdot p_{water} \qquad (2)$$

where:

$$S_{eff} = \frac{S - S_{res}}{S_{sat} - S_{res}} \qquad (3)$$

represents the degree of effective saturation (varying between 0÷1) while p_{water} is the sum of p_{steady} and p_{excess}. The former is the pore pressure at steady state (long term). The latter is the result of a deformation analysis (Brinkgreve, 2018).

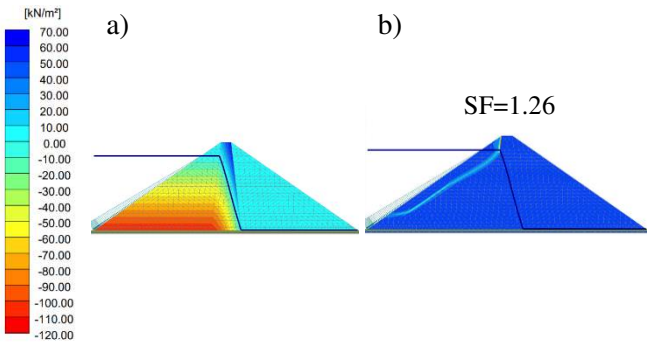

Figure 5. Contour of p_{active} and assessment of dam stability at the end of the filling phase.

The calculation of the safety factor was carried out through the so-called *c-φ reduction* analysis, a procedure that applies a reduction factor to both cohesion and friction of the soil until slope instability occurs (Dawson et al., 1999). Figure 5b shows the outcomes of the global stability analysis, which provided a safety factor SF equal to 1.26. The corresponding sliding surface lies completely within the upstream shell.

3.3 Drawdown from a static stage

The drawdown operation was imposed at the end of the impounding stage considering different drawdown scenarios in terms of water lowering rate and ratio. This latter quantity, h_w/H_w, is the ratio between the water level decrease and the total reservoir height as sketched in Figure 6. Five drawdown ratios, h_w/H_w, were considered (0.18, 0.36, 0.55, 0.73 and 0.91) (Figure 6). The condition of complete emptying of the reservoir (h_w=H_w=11m) was not considered since it is unlikely to occur in reality.

The drawdown stage was simulated through a fully coupled analysis *(Fully-coupled-flow-deformation procedure* in Plaxis2D) to account for soil skeleton and fluid coupling during the imposed drawdown. In particular, a time-dependent linear variation of the external water level on the upstream boundary of the dam was imposed.

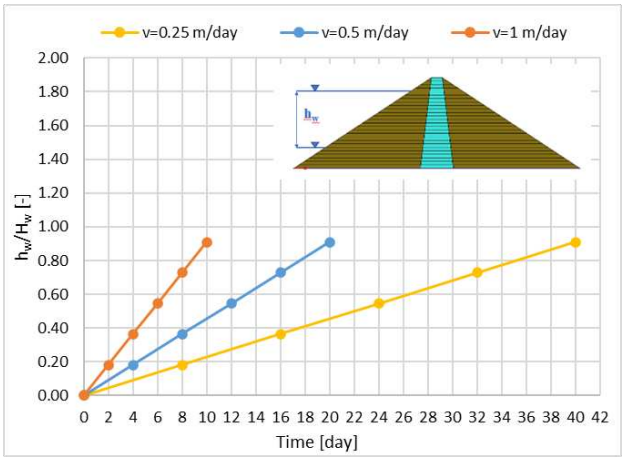

Figure 6. Drawdown scenarios imposed.

The distribution of pore water pressures inside the dam body was computed for three drawdown rates, corresponding to slow (0.25 m/day), intermediate (0.5 m/day) and rapid (1 m/day) emptying conditions.

With reference to the maximum drawdown height imposed (h_w=10m), Figure 7 shows the contours of pore water pressure for three different drawdown rates with the results of the global stability analysis after the target reservoir height has been reached. The results of the stability analysis have been provided in terms of global safety factor and the corresponding sliding surface, which now develops within the upstream shell of the dam.

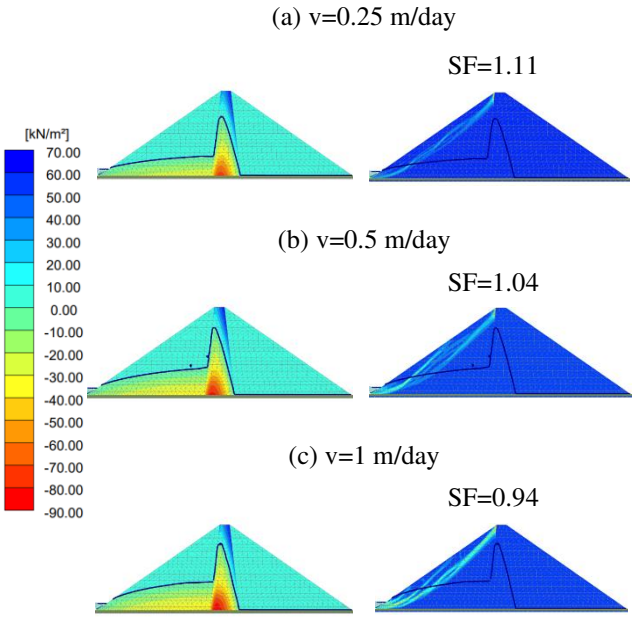

Figure 7. Contours of p_{active} at the end the drawdown with h_w=10 m and for drawdown rates of (a) 0.25 m/day, (b) 0.5 m/day, (c) 1 m/day. On the left, sliding surfaces and SFs provided by global stability analyses.

Independently from the rate adopted to lower the reservoir level, at the end of the drawdown stage the pore water pressures inside the core remain quite high and far from being in equilibrium with the external pressure of the reservoir. This response is emphasized when the drawdown velocity increases (Figure 7c) and dam response gradually tends to an undrained behaviour.

Figure 8 shows the decrease of the safety factor (SF) with increasing the drawdown ratio (h_w/H_w) for three different emptying rates considered in this study.

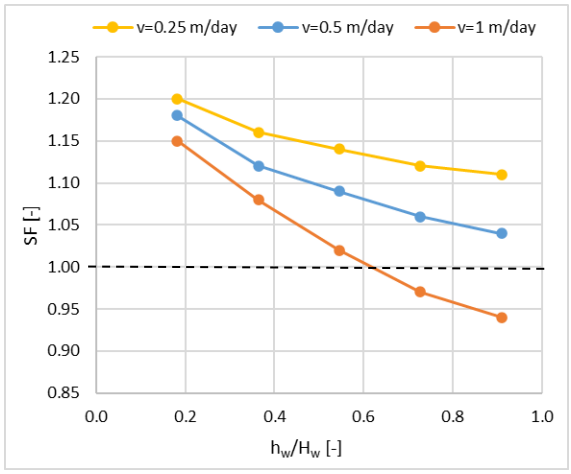

Figure 8. Stability safety factor (SF) against the drawdown ratio (h_w/H_w) for three different lowering rates.

Furthermore, as the drawdown rate increases (e.g. v=1m/day), a stronger decrease in safety factor is obtained up to global instability of the upstream shell for drawdown ratios, h_w/H_w, equal to 0.73 and 0.91.

This result highlights how crucial is the drawdown velocity also in the case of small zoned earth dams with the upstream shell made of sandy soils.

3.4 Dynamic stage

The dynamic stage was simulated with the impounding level fixed at its maximum height (H_w=11 m). At the bottom of the dam, an accelerometric input signal characterised by a peak acceleration a_{max}=0.1g and a predominant frequency f =4 Hz was applied in the horizontal direction. The accelerogram and the amplitude Fourier spectrum of the input signal are shown in Figure 10.

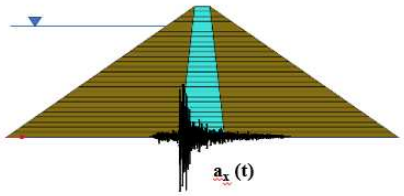

Figure 9. Dynamic phase simulation using Plaxis2D.

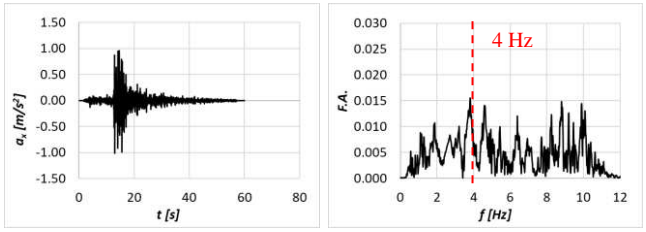

(a) (b)

Figure 10. Adopted input signal: (a) acceleration time history and (b) amplitude Fourier spectrum.

To properly simulate the initial soil damping, in addition to the hysteretic damping provided by the HS-small constitutive law, a material damping ξ = 1% was attributed to the dam soils through the Rayleigh damping formulation. The coefficients α and β, which respectively are proportional to the mass *[M]* and stiffness *[K]* matrix, were computed in correspondence of two target frequencies, f_1 and f_2, as proposed by Hudson et al. (1994) or Hash and Park (2002). In this case, f_1 was set equal to 5 Hz (almost equal to the first fundamental frequency of the dam) and f_2=15 Hz.

Figure 11 shows the seismic performance of the dam in terms of permanent horizontal, u_x, and vertical, u_y, displacements. Higher displacements may be observed on the upstream side of the dam with a maximum vertical displacement of about 0.28 m and a maximum horizontal displacement of about 0.24 m. The core, instead, denotes a less deformable response due to partial saturation occurring in a wider part of it. At the end of the seismic analysis, the slope stability analysis provided a safety factor of about 1.12 with sliding surface inside the upstream shell (Figure 12). Due to the earthquake, the safety factor of the dam is 9.6% lower than the value computed at the end of the first filling of the reservoir.

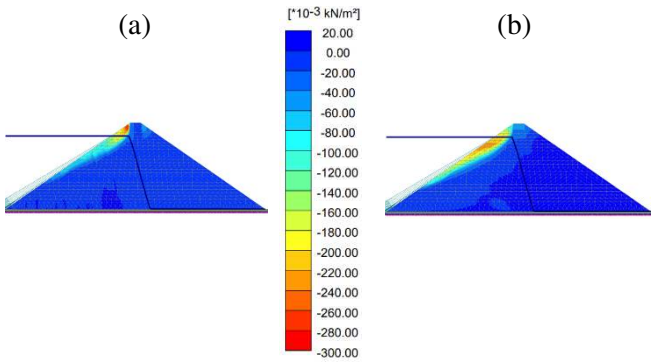

Figure 11. Contour of displacements at the end of the input signal: (a) vertical displacements, (b) horizontal displacements.

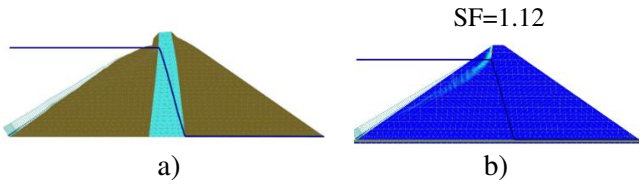

Figure 12. Deformed configuration at the end of the dynamic stage (a). Sliding surface and SF provided by global stability analysis (b).

3.5 Drawdown after a seismic stage

In this section, the performance of the small dam to an emergency drawdown imposed soon after the seismic stage discussed above, will be presented. In short, it was assumed that the dam suffered two critical events, the earthquake first and the fast drawdown later.

For brevity, the numerical results corresponding to two emptying rates (0.25 m/day and 1 m/day) and drawdown ratios of 0.55 and 0.91 (i.e. h_w equal to 6 m and 10 m) are shown in Figure 13 and 14.

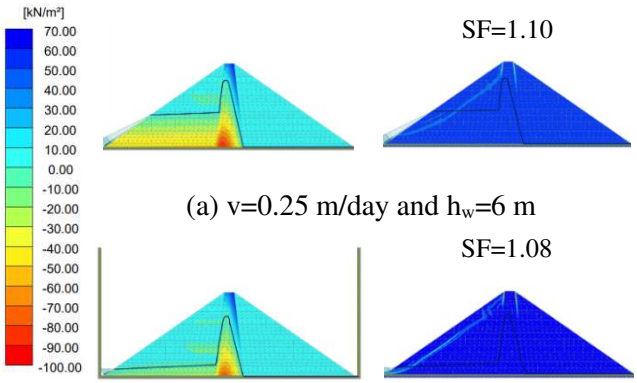

Figure 13. Contours of p_{active} at the end the drawdown scenario with h_w=6 m (a) and 10m (b) for the drawdown rate of 0.25 m/day. On the left, sliding surfaces and SFs provided by global stability analyses.

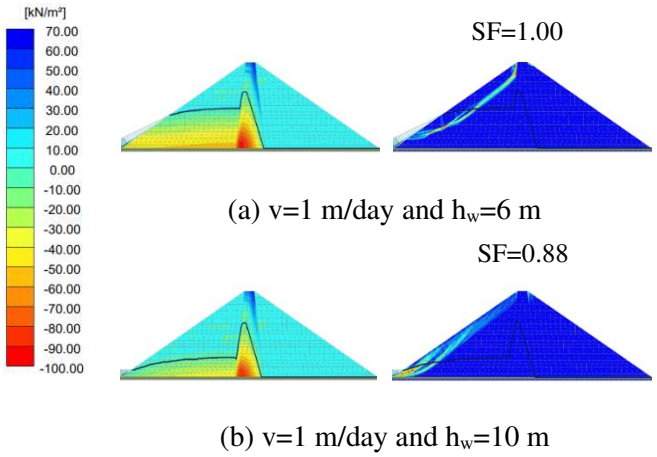

Figure 14. Contours of p_{active} at the end the drawdown with h_w=6 m (a) and 10m (b) for the drawdown rate of 1 m/day. On the left, sliding surfaces and SFs provided by global stability analyses.

Similarly to what observed in Figures 7 and 8 with reference to the drawdown inserted in the static stage of the dam, even for the drawdown carried out soon after the earthquake, the stability of the dam may be further reduced by the fast lowering of the water level combined to almost total emptying of the reservoir (i.e., v=1 m/s and h_w /H_w=0.91).

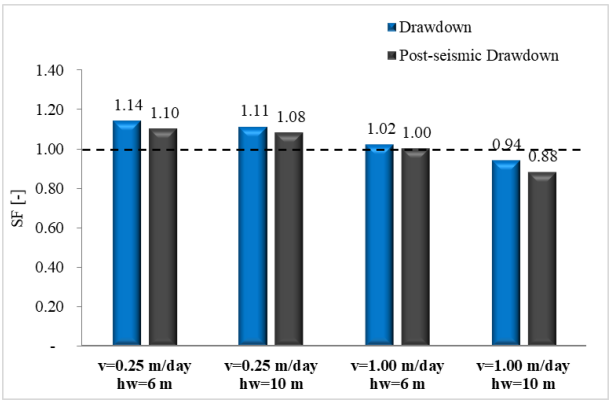

Figure 15. Safety factor (SF) at the end of the drawdown in case the reservoir lowering is imposed during a static stage (blue) or soon after a seismic stage (black).

The above outcomes are corroborated by the results provided in Figures 15 and 16, from which it is evident the negative role exerted by the seismic event on the stability of the small dam after the drawdown operation. As observed for large earth dams (Sica et al., 2019), the detrimental effects of rapid lowering operations can be further exacerbated by a previous seismic event.

This happens because the amounts of pore water pressures away from steady state conditions at the end of the drawdown process increases dramatically combining with the seismic-induced effects.

To provide operative indications to engineers or private owners of small dams, it could be stated that drawdown rates of no more than 0.25 m/day are safe enough as the computed global safety factors were higher than

one for all levels of reservoir emptying, even after the seismic stage.

Conversely, with a faster drawdown of 1 m/day, dam stability is guaranteed only with a partial emptying of the reservoir (h_w /H_w= 0.55). If a previous earthquake occurred, this drawdown rate should be avoided since SFs much less than one were obtained.

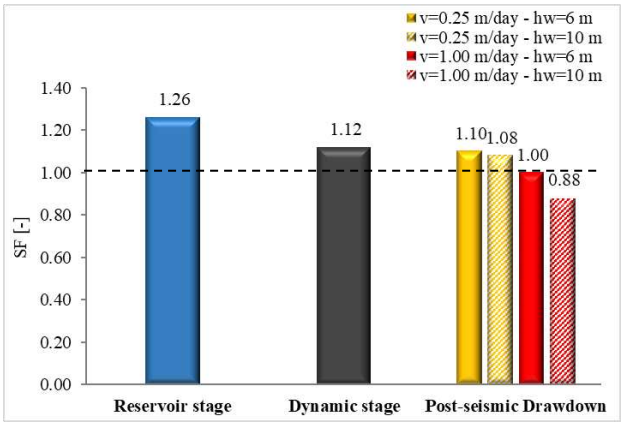

Figure 16. SF at the end of the main stages of dam lifetime and at the end of different drawdown scenarios.

4 CONCLUSIONS

The paper illustrated the performance of a small zoned earth dam which represents a dam typology often in charge of private owners or peripheral agencies, which are not subjected to the same strict controls required for large dams.

The numerical study was carried out through the f.e. software Plaxis2D, by simulating different drawdown scenarios both during the ordinary static stages of the dam lifetime and soon after the simulation of a seismic stage. The goal was to assess the proper drawdown procedures to avoid global instability inside the dam.

The analyses were performed by a three-phase formulation to account for partial saturation of the dam soils. An elasto-plastic constitutive model (HS-small), able to describe the soil nonlinear and hysteretic behaviour in a wide range of strains, was assigned to dam core and shells.

Different drawdown rates and emptying ratios were simulated. As the drawdown rate and ratio increase, the dam safety factor with respect to global instability reduces dramatically. Slope instability (SF<1) might occur for the exceptional velocity of 1 m/day if almost complete emptying of the reservoir is reached.

If the drawdown follows an earthquake stage, lower safety factors were computed in the dam and safety of the slopes is guaranteed only with a drawdown velocity not higher than 0.25 m/day.

Nevertheless, all the computed critical sliding surfaces were found to be contained in the upstream shell without affecting the clayey core, that is, the dam watertightness.

As a final note, the outcomes of the present study should not be extended to other typologies of small dams. Further computations are needed to ascertain the role of different properties assigned to the dam soils (in particular, the adopted retention curves) and more input signals to simulate the seismic response of the dam.

5 REFERENCES

Alonso, E., Pinyol, N. 2009 Slope stability under rapid drawdown conditions. Barcelona: Universitat Politecnica de Catalunya.

Alonso, E., Pinyol, N. 2016. Numerical analysis of rapid drawdown: applications in real cases. Water Sci Eng. 9(3), 175-182

Brinkgreve, R.B.J. 2018. PLAXIS 2D Manuals. General Information. Tutorial Manual. Reference Manual. Material Models Manual. Scientific Manual. *Delft University of Technology & PLAXIS. ISBN13.978*(90). 76016.

Dawson, E.M., Roth, W.H., Drescher, A. 1999. Slope stability analysis by strength reduction. *Geotechnique, 49 (6)*, 835-840.

Hudson, M., Idriss, I.M., Beirkae, M. 1994. QUAD4M User's manual. *A computer program to evaluate the seismic response of soil structures using finite element procedures and incorporating a compliant base.*

Hashash, Y.M., & Park, D. 2002. Viscous damping formulation and high frequency motion propagation in non-linear site response analysis. *Soil Dynamics and Earthquake Engineering*, 22(7), 611-624.

Sica, S., Pagano, L., Rotili, F. 2019. Rapid drawdown on earth dam stability after a strong earthquake. *Computers and Geotechnics*, 116, 103187.

Zedan, A.J., Faris, M.R., Abdulsattar, A.A. 2018. Slope Stability of an Earth Dam during Drawdown Conditions (KHASA-CHAI Dam) as a Case Study. *International Journal of Engineering and Technology*, 7(37), 17-21.